ISET Journal of Earthquake Technology, Paper No. 506, Vol. 46, No.3-4, Sept.-Dec. 2009, pp. 131–138

SIMULATION OF STRONG GROUND MOTIONS OF WENCHUAN EARTHQUAKE BY STOCHASTIC FINITE-FAULT METHOD

Wang Guoxin Shi Jiaping

State Key Laboratory of Coastal and offshore Engineering
Dalian University of Technology, Dalian 116024, China

ABSTRACT

Wenchuan earthquake (Ms=8.0, May 12, 2008, Sichuan, China) had caused great losses to both in life and property. The paper computes the accelerograms of Wenchuan strong earthquakes by Stochastic Finite-fault Method and obtained isolines of peak ground acceleration The study will provide reasonable interpretation of the cause and degree of structural destruction caused by strong ground motions during this event. It will improve the stochastic finite-fault method by incorporating structural aseismic capability.

KEYWORDS: Wenchuan; Stochastic Finite-Fault Method; Near-Fault Strong Ground Motion

INTRODUCTION ABOUT WENCHUAN EARTHQUAKE

The Wenchuan earthquake had a magnitude of 8.0 M_s or 7.9 M_w according to the China Earthquake Administration (CEA). The epicenter was in Wenchuan County (31.0ºN, 103.4ºE), 80 km west-northwest of the provincial capital city of Chengdu, with its main tremor occurring at 14:28:01.42 CST (06:28:01.42 UTC), on Monday May 12, 2008. This earthquake was felt as far as Beijing (1,500 kilometers away) and Shanghai (1,700 kilometers away), where office buildings swayed with the tremor. The earthquake was also felt strongly in nearby counties, the highest MMI is Ⅺ in Beichuan. It is the deadliest and strongest earthquake to hit China since the 1976 Tangshan earthquake.

This earthquake occurred along the long and complex Longmenshan fault consisted of three parallel faults and several transversal faults (Figure 1), resulted due to thrusting along the border of Indo-Australian and Eurasian Plate. The rupture was initialed at the middle of the fault known as Yingxiu-Beichuan fracture and was lasted close to 120 sec, with major energy released during first 80 sec. Starting from Wenchuan, the rupture propagated at an average speed of 3.1km/s towards north east direction, rupturing a total length of about 300 km. Maximum displacement of the fault was 9 meters. The relative motion between the India and Eurasian plate causes large scale structural deformation inside the Asian continent, resulting crustal thinning of the Qinghai-Tibet Plateau, uplift of its landscape and an eastward extrude. Near the Sichuan Basin, Qinghai-Tibet Plateau's east-northward movement meets with strong resistance from the South China Block, causing a high degree of stress accumulation in the Longmenshan thrust formation. This finally caused a sudden dislocation in the Yingxiu-Beichuan fracture, leading to the violent earthquake of Ms 8.0 (Reference 3, 2009).

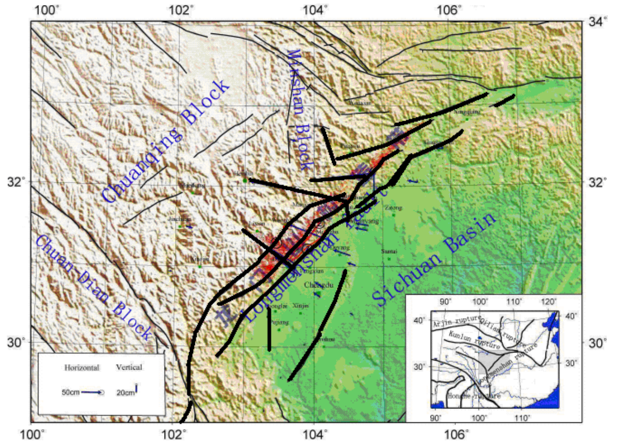

Fig. 1 Longmenshan fault (from the website of China Earthquake Info)

The purpose of this paper is to estimate the strong ground motion distribution, which will be helpful in understanding the cause and analyzing reason and degree of structural destruction due to this event.

STOCHASTIC FINITE-FAULT SIMULATING METHOD

Moment Rotation Relation

2.1 Source Parameters

2.1.1 Source Spectral Model

Source spectral model $S(M_0, f)$ is expressed as follows (Wang, 2001), which is the modification to traditional ω^2 model by linking the coefficient *a* and *b* with magnitude in order to reduce obvious "sag" phenomenon in transitional frequency range between low and high frequencies as the magnitude increasing.

$$S(M_0, f) = \frac{M_0}{\left[1+\left(f/f_0\right)^a\right]^b} \tag{2.1}$$

where, M_0 is seismic moment, f represents frequency, f_0 is corner frequency, coefficient $a = 3.5- 0.3M$, $b=2/a$, which were estimated by strong ground motion recordings.

2.1.2 Main Source Size

Kanamori and Anderson (1975) suggested a theoretical relation between the rupture area, *S*, stress drop, $\Delta\sigma$, and seismic moment M_0 of an earthquake based on seismological theory,

$$\log M_0 = 1.5\log S + \log\Delta\sigma + \log C \tag{2.2}$$

where, M_0 can be computed from moment magnitude M_W, *C* is the constant related to the fault type as suggested by Hanks and Kanamori (1979):

$$\log M_0 = 1.5M_W + 16.1 \tag{2.3}$$

According to the definition of M_0, it is known that:

$$M_0 = \mu \ \ SD \tag{2.4}$$

The value of $\Delta\sigma$ could be expressed as

$$\Delta\sigma = C'u\frac{\overline{D}}{L} \tag{2.5}$$

where, $\overline{D}$ is the mean slip on fault, shear modulus $u = 3.1\times10^{11}$. The factor C' is related with the fault length, L, as

$$\begin{cases} C' = \dfrac{7\pi}{16},\ L = r & \textit{disk rupture} \\ C' = \dfrac{16}{3\pi},\ L = W & \textit{thrust fault} \\ C' = \dfrac{2}{\pi},\ L = W & \textit{strike slip fault} \\ C' = \dfrac{4(\lambda+\mu)}{\pi(\lambda+2\mu)},\ L = W & \textit{downdip slip fault} \end{cases} \tag{2.6}$$

r is the disk radius, W the fault width, λ is Lama constant, L could be expressed as:

$$\log L = 0.5 M_W + 5.4 + \frac{2}{3}\log C + \log C' - \frac{1}{3}\log \Delta\sigma \tag{2.7}$$

The parameter C in equation (2.2) can be expressed as

$$C = \begin{cases} \dfrac{16}{7\pi^{3/2}} = 0.4105 & \textit{disk rupture} \\ \dfrac{3\pi}{16} = 0.589 & \textit{thrust fault} \\ \dfrac{\pi}{2}\left(\dfrac{W}{L}\right)^{1/2} & \textit{strike slip fault} \\ \dfrac{\pi(\lambda+2\mu)}{4(\lambda+\mu)}\left(\dfrac{W}{L}\right)^{1/2} & \textit{downdip slip fault} \end{cases} \tag{2.8}$$

These theoretical equations can be used to calculate the rupture radius for disk fault model or rupture width for rectangle fault model.

For a rectangle fault model, the rupture area $S = L \times W$, hence, by substituting the value of S into equation (2.4) and combine it with equation (2.3), (2.5) and (2.7), following equations could be induced

$$\log L = 0.5 M_w + 5.3 - \frac{4}{3}\log C - \log C' - \frac{1}{3}\log \Delta\sigma \tag{2.9}$$

Substituting equations (2.5) to (2.7), the relation between the parameter $\overline{D}$ and *Mw* can be obtained as follows

$$\log \overline{D} = 0.5 M_W + 5.4 + \frac{2}{3}(\log C + \log \Delta\sigma) - 11.5 \tag{2.10}$$

The detail of deduction is shown in Wang (2004), therefore not repeated here.

2.1.3 Subsource Parameters

The preliminary requirement dividing the main source into various subsources is that the cumulative energy released by the subsources should be equal to that released by the main source. This will insure that the seismic moment summation from all subsources should be equal to the total seismic moment from main source. Wang (2001, 2008) suggested that there exists one suitable subsource size, ***ΔL***, correspond to subsource magnitude ***Mz*** that could simulate better accelerogram once the event magnitude (*M*) and total rupture length (*L*) of the fault are known. Wang (2001, 2008) used the following equation based on previous research results (Beresnev,1997; Shi Yucheng, Chen Houqun, 2005; Tao Xiaxin, Wang Guoxin, 2003) to compute source size.

$$\log(\Delta L) = \log(L) - 0.5(M - M_z) \tag{2.11}$$

The subsource size obtained from above equations corresponds to the subevent magnitude and could be treated as point source. Once ***ΔL*** is determined then the seismic moment of each subsource could be estimated, and thus, the subevent number ***Ne*** could also be obtained from main event seismic moment.

Subevent seismic moment

$$M_e = \Delta\sigma \cdot A \cdot \Delta L \tag{2.12}$$

Subevent number

$$N_e = \frac{M_0}{M_z} \tag{2.13}$$

So the accelerogram *a(t)* caused all subevents could be generated by superposing the initial accelerograms with appropriate delay from all subevents.

$$a(t) = \sum_{i=1}^{N_L}\sum_{j=1}^{N_W} a_{ij}(t + \Delta t_{ij}) \tag{2.14}$$

where N_L and N_W is subevent number along fault length and width respectively, and $N_L \times N_W$ =*Ne*, *Ne* is the total subevent number; Δt_{ij} represents the time delay of wave propagating from the fixed starting point of rupture on fault to *ij*th subsource center and then to expected analyzing site, $a_{ij}(t)$ is the accelerogram caused by *ij*th subsource.

2.2 Modeling

We modeled the area bounded by 98ºE to 112ºE, 28ºN to 37ºN, which is around the Longmenshan fault.

The fault dimension of Wenchuan Earthquake is about 320km×30km, which could be divided into 48 subsources with the size of 20km×10km in this study according to equation (2.11).

The seismic moment of each subsource therefore can be estimated as (Beresnev, 1997):

$$M_e = (\Delta\sigma)S(\Delta L) = (\Delta\sigma)(W\Delta L^2) = 1.0\times10^{19}(Nm)$$

and the number of subevent will be

$$N_e = \frac{M_0}{M_z} = \frac{1.4\times10^{21}}{1.0\times10^{19}} = 140$$

Thus, there are 48 subsources and 140 subevents that could represent the actual earthquake, which are distributed on fault plane, and indicates that slip distribution may be different in each subsource. Normally there are more subevents around hypocenter than the edge of the fault. The subevents distribution is shown in Figure 2. However, the actual distribution may be different because of inversion results. The effect of distribution is not large as observed from the sensitivity analysis on source parameter variation. The hypocenter of Wenchuan earthquake is treated as starting point of fault rupture process.

1	3	4	5	5	4	4	3	3	3	3	2	2	2	1	1
2	3	4	5 ★	5	4	4	3	3	3	3	2	2	2	1	1
2	3	4	5	5	4	4	3	3	3	3	2	2	2	1	1

hypocenter

Fig. 2 Subsource distribution

2.3 Parameter Estimation

The various seismological parameters of main and subsources, shown in Table 1, could be estimated by the method introduced above, including the exact fault length, width, depth and striking angle as indicated in it. The geological data around Wenchuan region are also listed in Table 2. The nonlinear attenuation assumed to be frequency independent.

Table 1: Source Parameters

Source Parameters	
Event time	14:28pm, May.12, 2008
Epicenter	30.94°N; 103.47°E
Hypocenter depth(km)	14
Breaking mode	unilateral, toward NE
Fault type	Dextrorotation strike fault
Striking and dip angles	70°/NE; ∠40°
Main fault dimension(length×width)(km)	320×30
Subfault dimension(length×width)(km)	20×10
Subsource number	48
Subevent number	140
Fault length(km)	3~20
Main event seismic moment M_0(N·m)	1.4×10^{21}
Subevent seismic moment Me(N·m)	1.0×10^{19}
Moment magnitude Mw	8.3

Mean slip (m)	1.5
Stress drop (Pa)	2.5×10^{6}
Shear velocity β(km·s-1)	3.5
Breaking velocity $v_r(km\cdot s^{-1})$	3.0
Rupture duration (s)	120

Table 2 Geological parameters

Upper depth(m)	Thickness (m)	Shear vel. (m/s)	Density (kg/m3)	Q
0	100	1500	2200	150
100	1000	2800	2500	200
1100	5000	3200	3000	350
6100	50000	3600	3200	400

2.4 Data and Result Analysis

2.4.1 Data

In order to compare the difference in theoretical and real situations, and to illustrate the reasons that cause such differences, we simulate the accelerogrmas at two seismological stations, e.g., Chengdu (104.06ºE、30.67ºN) and Lanzhou (103.50ºE、36.03ºN) where the recorded time histories are available. Figure 3 shows random accelerograms (*a* and *b* respectively) simulated for Chengdu and Lanzhou stations. The recorded accelerograms at these stations are shown in figure 4, which indicate that the PGA is about 610cm/s^2 in Chengdu station and 80 cm/s^2 in Lanzhou station respectively.

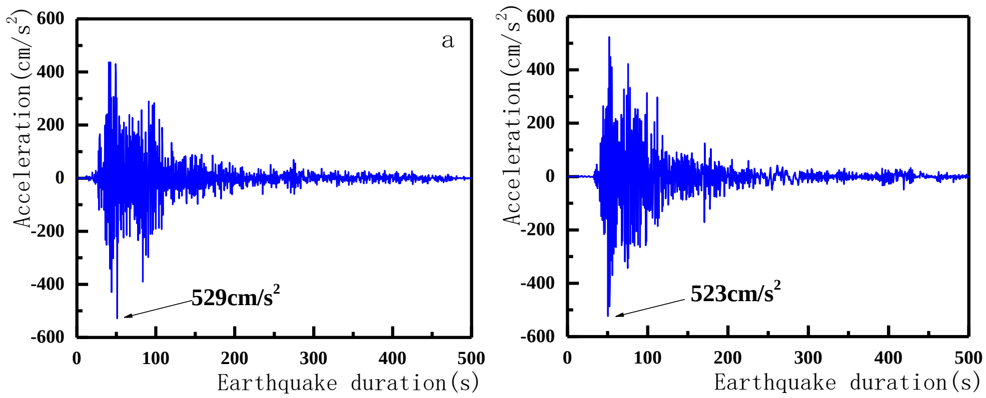

(3-1)

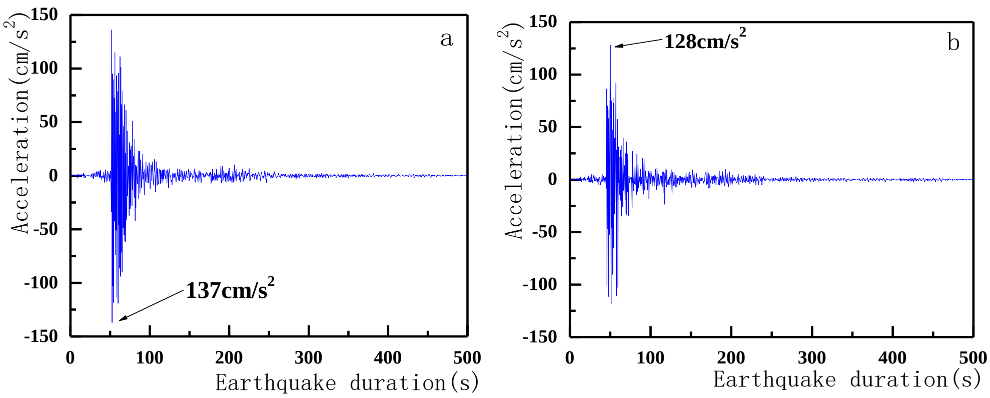

(3-2)

Fig. 3 Simulated accelerograms in Chengdu(3-1) and Lanzhou(3-2)

It is observed from Figure 3 and Figure 4 that the simulated as well recorded time series are of relatively higher amplitude in near fault region with long duration. The simulated and recorded accelerograms are comparable both in amplitudes and wave forms showing acceleration variation process during earthquake, which indicate that the method and parameters we adopted are suitable for analyzing the strong ground motion variation for such a strong earthquake.

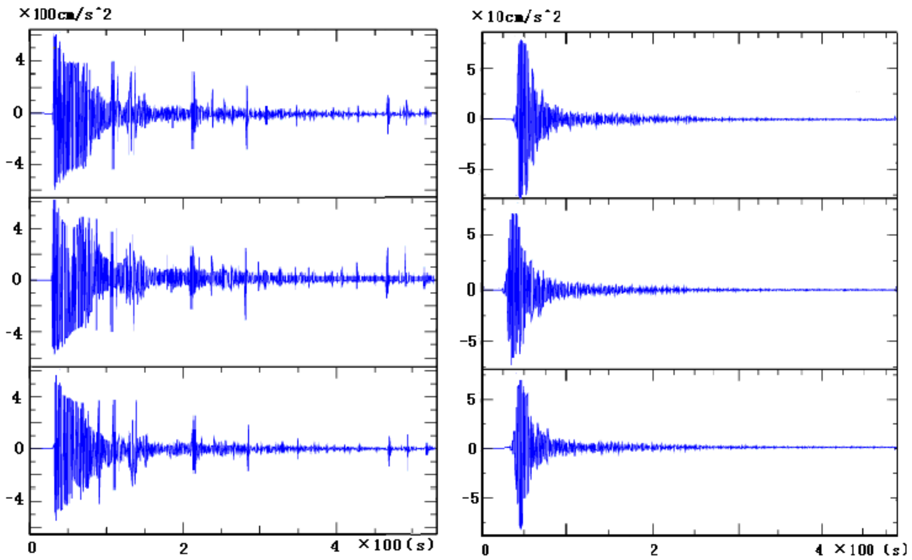

Chengdu station (epicenter distance 64km) Lanzhou station (epicenter distance 567km)

Fig. 4 Recorded accelerograms in Chengdu and Lanzhou (upper, middle and bottom is two horizontal and one vertical accelerogram respectively)

2.4.2 Result Analysis

To study the spatial variation of PGA in Wenchuan and surrounding region, we calculated the accelerogram from 98º to 112ºE and 28º to 37ºN with grid spacing of 0.2º╳0.2ºand estimated the PGA isolines (Figure 5), It is observed that PGA distribution is not symmetrical about the fault-axes. It is greater than 600 cm/s^2 with the mean PGA about 400 cm/s^2 alone 300km long fault. The PGA is higher than 300 cm/s^2 within about 100km perpendicular to the fault, which causes substantial disaster. Meanwhile, the directivity effect in figure 5 is very typical, especially in near fault region, the large expanding trend of PGA is formed direction but small one in SW direction as the fault rupturing toward NE. All of these preliminary phenomena could be presented by our simple and easy method reasonably.

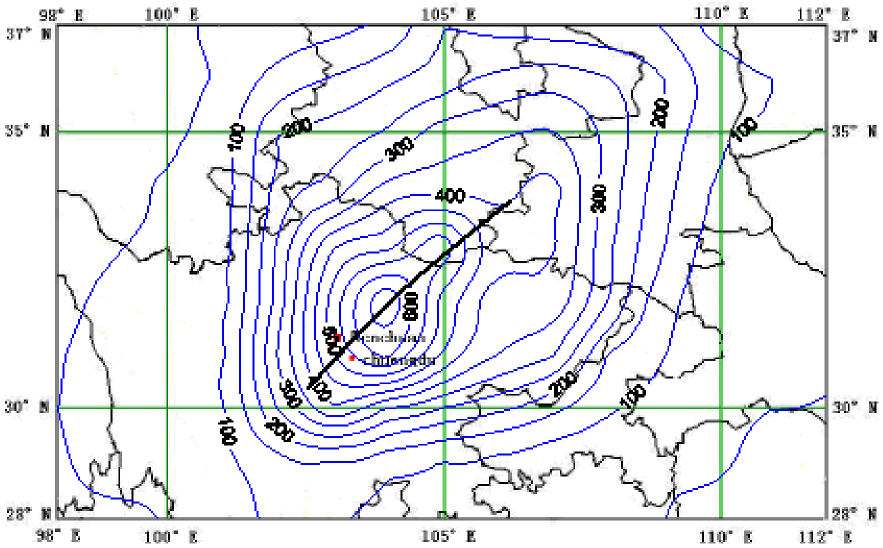

Fig. 5 Estimated PGA isolines of Wenchuan earthquake

The isolines from recordings of this earthquake in EW direction are shown in figure 6, and the recorded PGA is 632.9cm/s^2 on it. It could be found after comparison figure 5 and 6 that both of them are similar basically from the amplitudes to the distribution trend, so the practical situation could be represented if the method and parameters are selected properly.

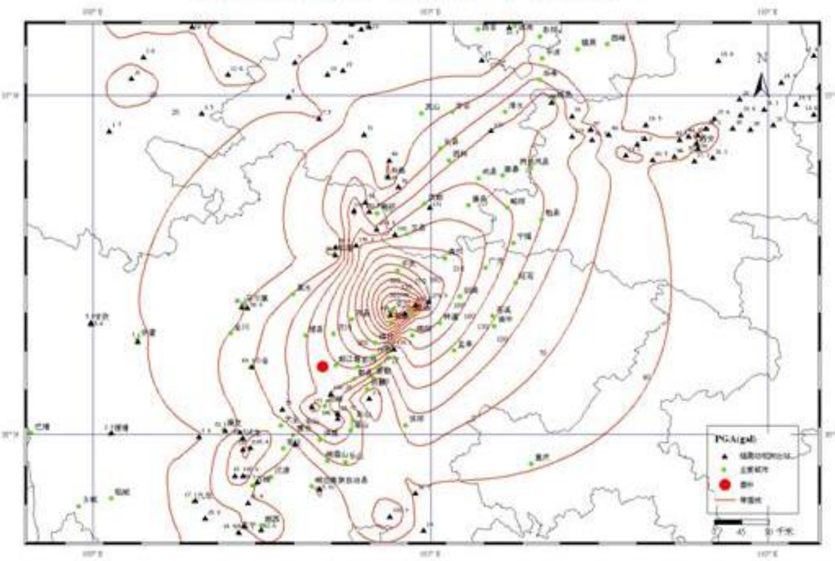

Fig. 6 Recorded PGA isolines of Wenchuan earthquake in EW (Reference 4, 2009)

CONCLUSIONS

Following conclusions can be drawn from the analysis results of the results:

1. This earthquake is characterized by large affecting region, huge energy release, longer fault size, larger PGA and longer duration. All these characters could be simulated reasonably well by our method;
2. The highest PGA is not at the epicenter area (Wenchuan) but at Beichuan in Mao county. The directivity effect has been found to be dominate during this earthquake, which causes huge casualty and economic losses in these regions;
3. The PGA distribution is not symmetrical around the fault, this indicates the complexity of wave propagation and local site effect on ground motions;
4. The PGA isolines from simulated accelerogram and recordings indicate that theoretical methods could represent the similar PGA distribution between them if the methods and parameters are chosen properly. The stochastic finite fault method is one of the simple and easy tools.

Several problems still need to be solved further in future work to predict accurately the expected ground motions

1. It is known the earthquake source may not be treated as "point" source when magnitude is larger, which is the case for Wenchuan earthquake. So although relatively small magnitude for each subsource has been adopted in simulating accelerograms in our suggested finite-fault method in order to match point source morel, some other related aspects still need to be improved to make the simulated results to match the recorded data, especially for large magnitude and middle-far distance range;
2. The uncertainties on estimated physical parameters adopted in analyzing process, stress drop, for example, have obvious effect on results. So how to reduce these effect is our main target for future study;
3. The assumption of uniform geological distribution for larger region may be not be suitable for modeling the wave propagation, as we did in our analysis. Thus the simulated results sometime differ from the recorded ones.

REFERENCES

1. Beresnev, I.A. and G., Atkinson (1997). "Modeling Finite-Fault Radiation from the ω' Spectrum", BSSA, Vol. 87, No. 1, pp. 67-84.

2. Hanks, Thomas C. and Hiroo, Kanamori. (1979). "A Moment Magnitude Scale". Journal of Geophysical Research, Vol. 84, No. B5, pp. 2348-2350.
3. http://www.cea.gov.cn/manage/html/8a8587881632fa5c0116674a018300cf/_content/08_05/30/1212119940937.html
4. http://www.csi.ac.cn/manage/html/4028861611c5c2ba0111c5c558b00001/_content/08_06/06/1212732534049.html
5. Kanamori, H. and Anderson, D.L. (1975). "Theoretical Basis of Some Empirical Relations in Seismology", BSSA, Vol. 65, pp. 1073-1095.
6. Shi Yucheng, Chen Houqun, Li Min and Lu Yuxia. (2005). "The Study and Application of Stochastic Finite Faults Method in Ground Motion Synthesizing", Earthquake Engineering and Engineering Vibration, Vol. 25, No. 4, pp. 18-23.
7. Tao Xiaxin and Wang Guoxin. (2003). "Rupture Directivity and Hanging Wall Effect in Near Field Strong Ground Motion Simulation", Acta Seismological Sinica, Vol. 25, No. 2. pp. 191- 199.
8. Wang Guoxin and Shi Jiaping. (2008). "Study and Simulation on Near-site Strong Ground Motions". Seismological Research of Northeast China, Vol. 24, No. 2. pp. 4-10.
9. Wang Guoxin (2001). "Study on Strong Ground Motions", Ph.D dissertation, Institute of Earthquake Mechanics, CEA (in Chinese)
10. Wang Haiyun. (2004). "Finite-fault Model for Predicting Near Site Ground Motion", Ph.D dissertation, Institute of Earthquake Mechanics, CEA(in Chinese)